The influence of precursors on optical properties of carbon nanodots synthesized via hydrothermal carbonization technique

Kamonwan AUP-NGOEN[1,*], Mai NOIPITAK[1], Nant NAMMAHACHAK[2], Sutatch RATANAPHAN[2], Chatwarin POOCHAI[3], and Adisorn TUANTRANONT[3]

[1] *Materials and Nondestructive Testing Laboratory, King Mongkut's University of Technology Thonburi (Ratchaburi), Chom Bueng, Ratchaburi 70150, Thailand*
[2] *SimDscience Laboratory, KMUTT Surface Engineering Laboratory, Dept. of Tool and Materials Engineering, Faculty of Engineering, King Mongkut's University of Technology Thonburi, Thung Khru, Bangkok 10140, Thailand*
[3] *Graphene and Printed Electronics for Dual-Use Applications Research Division (GPERD), Nation Security and Dual-Use Technology Center (NSD), Nation Science and Technology Development Agency (NSTDA), Phahon Yothin Road, Klong Luang, Phathum Thani 12120, Thailand*

Corresponding author e-mail: kamonwan.aup@kmutt.ac.th

Abstract

Carbon nanodots (CDs) have drawn much attention due to their potential applications in optoelectronic devices, bioimaging, biosensor, and hole transporting materials for a perovskite solar cell. In this work, CDs were synthesized from natural mono- or disaccharide precursors (glucose, fructose, and sucrose) via a hydrothermal carbonization technique with the addition of ethanol or acetone. Structural and morphology of CDs were investigated using transmission electron microscopy and selected area electron diffraction. The average particle size of CDs was in the range 4.86-9.99 nm. The optical properties of CDs were characterized by UV-Visible spectroscopy and Fluorescence spectroscopy. The absorbance intensity of CDs increased with increasing precursor concentration. In the present work, the influences of precursors with addition of acetone on the optical properties of CDs were investigated and discussed the possible reason. The results revealed the improvement on the absorbance of CDs synthesized using a sucrose precursor. Additionally, the CDs showed the shifted fluorescence peaks when excited at different excitation wavelengths, indicating the excitation wavelength-dependent emission properties of CDs. FTIR spectra show that the CDs surface containing double bonded oxygen functional groups (C=O) formed during the hydrothermal carbonization of fructose and sucrose precursor, which is not found in glucose-derived CDs. Oxidation, reduction potentials and band gaps of CDs were also analyzed using the cyclic voltammograms (CV). The as-prepared CDs in diluted ethanol presented slightly difference of the HOMO and LUMO energy when compared with the CDs synthesized in diluted acetone.

1. Introduction

Carbon nanodots (CDs) with a quasi-spherical shape in nanoscale represent a promising material due to their unique properties, such as low cost, low toxicity, high solubility, and biocompatibility [1]. The sp^2 bonding of carbon atoms in CDs affords them extraordinary properties, such as charge carrier mobility, stable fluorescence properties, tunable light absorption and emission properties which make them attractive for a range of applications in bioimaging, biosensor, modifying materials, optoelectronic devices and solar cell [2-7]. Graphitic CDs have been synthesized by different approaches, such as electrolysis synthesis, plasma process, microwave heating method, ultrasonic assisted precipitation, and hydrothermal carbonization [6-11]. Among the several techniques, a facile hydrothermal carbonization is a simple method and has been widely studied.

Research on CDs has been at the forefront over the past several years. These efforts include providing insight into the key mechanism of CDs fluorescence properties. Many researches show that the optical properties of CDs depend on the recombination of confined electron-hole pairs of conjugated π electron within the carbon-core state, although recent studies suggest that the presences of different surface functional groups of CDs are the most probable origin of variation in fluorescence properties [12]. The exploration of possibility mechanism has been extensively conducted through the surface passivation of CDs as well as the carbon source enhanced the fluorescence intensity [12-14]. Most research reported the excitation wavelength-dependent emission properties of CDs were due to the size differences of CDs or the presence of various surface functional group. Rajneesh et al. reported the role of different functional group on the fluorescence properties of carbon dot [15]. By tuning of the functional groups, the fluorescence properties and emission wavelength could be tuned. Recently, Nikolaos et al. showed that the solvents used to suspend the synthesized carbon nanodots also

The influence of precursors on optical properties of carbon nanodots synthesized via hydrothermal carbonization technique

89

correlate to the optical properties of CDs in which the emission changes in different solvents [16]. Liman et al. reported that the optical properties of CDs depend on their surface states and emission peak may be resulted from the structure of precursor [17]. While these previous studies demonstrated that the excitation wavelength-dependent emission properties of CDs are strongly influenced by the surface functional groups of CDs and the solvents, the influences of precursors on the CDs fluorescence properties is still not clear and remains under research.

In an attempt to investigate the influence of precursors on the optical properties of CDs, the monosaccharide and disaccharide sugars (glucose, fructose and sucrose) have been utilized as precursors for the hydrothermal carbonization of CDs with the addition of ethanol or acetone. Transmission electron microscopy (TEM), selected area electron diffraction (SAED), UV– Visible spectroscopy (UV- Vis) and fluorescence spectroscopy (FL) were used to characterize the structure and optical properties of the synthesized CDs. Fourier transform infrared spectroscopy (FTIR) were used to investigate the functional groups and chemical bonding in the samples.

2. Experimental

2.1 Synthesis of CDs

CDs were synthesized from different precursors (glucose, fructose and sucrose) through a facile one-step hydrothermal carbonization. Each of CDs precursors was dissolved in a diluted 50%v/v ethanol or a diluted 50%v/v acetone solution with deionized water (see Table 1.), then the mixture was added into a Teflon- lined stainless steel autoclave with 80% filling of total capacity and heated at 160°C for 6 hours. After cooling to a room temperature, this brown solution was dialyzed to remove the residual sugar precursor against deionized water in a dialysis membrane for further characterization.

2.2 Characterization of CDs

The particle size and dispersity of the synthesized CDs were collected using a transmission electron microscope (JEM- 2011 TEM, JEOL) with 200 kV. TEM grids were prepared by placing diluted and well sonicated sample solution on a carbon coated copper grid. The sample solution was evaporated at room temperature. Ultraviolet- visible (UV-Vis) absorption spectra of CDs were obtained using UV-Vis spectro-photometer Genesys 10S, Thermoscientific). The spectra were collected using 10 mm path length quartz cuvette. Fluorescence (FL) excitation and emission spectra were measured in a microcell with 1 cm path length using a Fluorescence spectrophotometer (Infinite 200, TECAN). The Fourier transform infrared spectra of CDs were obtained using a Fourier transform infrared spectrometer (Shimadzu Europe - IR Prestige-21) in order to examine

the chemical bonding and surface functional group of CDs. For electrochemical measurement, a typical three- electrodes consisted of a glassy carbon disc with diameter of 1 mm (working electrode), a platinum rod with diameter of 1 mm (counter electrode), and a commercial Ag/AgCl in 3 M KCl electrode (reference electrode) were connected to a potentiostat (Metrohm, Eco Chemie Autolab PGSTAT30) operated with NOVA 1.11 software. A mixture solution, containing 50 ml of 2 M H_2SO_4 mixed with 10 ml sample solution, was used as electrolyte solution (60 ml). Before measurement, the electrolyte solution was ultrasonicated for 30 min. Cyclic voltammetry (CV) was performed in a potential range of 0-1 V with a scan rate of 50 mVs^{-1} at room temperature.

Table 1. Preparation conditions of CDs

| Samples	Precursors	%Weight of precursor	Diluted solution (%vol/vol)
SCET2	Sucrose	2%	50% Ethanol
SCET4	Sucrose	4%	50% Ethanol
SCET6	Sucrose	6%	50% Ethanol
SCET8	Sucrose	8%	50% Ethanol
SCAC2	Sucrose	2%	50% Acetone
FTAC2	Fructose	2%	50% Acetone
GCAC2	Glucose	2%	50% Acetone

3. Results and discussion

### 3.1 Structural and morphology characterization of CDs

The preparation of CDs through hydrothermal carbonization is shown in Figure 1. The hydrothermal treatment carbonizes the precursor in the presence of diluted 50%v/v ethanol or diluted 50%v/v acetone solution. Figure 2 presents TEM images of the CDs synthesized using different %weight of a sucrose precursor with the addition of ethanol. The TEM images show CDs which are surrounded by an amorphous carbon matrix. Increasing of %weight of the precursor resulted in the aggregation of CDs.
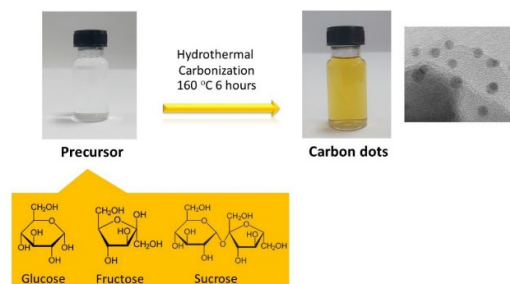
**Figure 1.** Schematic illustration of the preparation of CDs.

Aup-ngoen, K., et al.
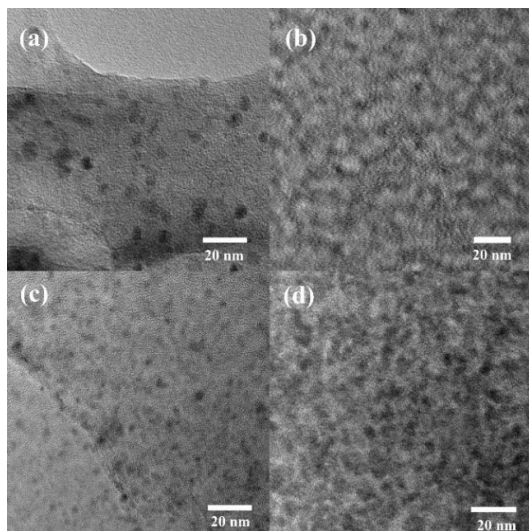
Figure 2. TEM images of CDs synthesized using a sucrose precursor with (a) 2%wt (b) 4%wt (c) 6%wt and (d) 8%wt in diluted ethanol.
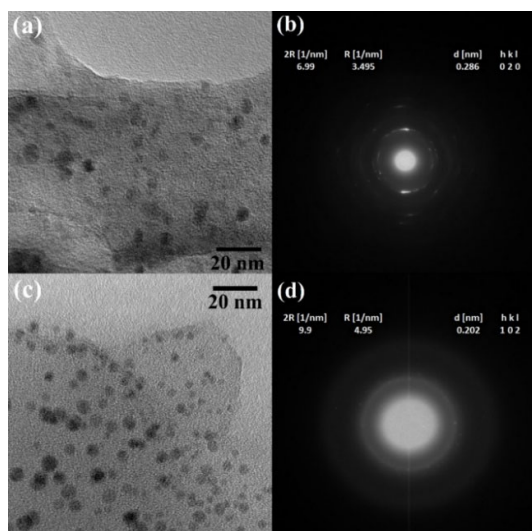
Figure 3. TEM images and SAED patterns of CDs synthesized using a 2%wt sucrose precursor in (a) diluted ethanol and (b) diluted acetone.

Figure 3 displays TEM images and SAED patterns of CDs prepared from a sucrose precursor diluted in different solvent. The SAED patterns clearly reveal a diffused ring pattern, suggesting the crystalline nature of (020) and (102) plane for CDs synthesized in diluted ethanol (SCET2) and diluted acetone (SCAC2), respectively [18- 19]. While these CDs have well-dispersed nano-size and crystalline structure, the average size of CDs synthesized with the addition of ethanol and acetone is 5.8 ±1.07 nm and 5.0±1.19 nm, respectively. CDs (FTAC2 and GCAC2) prepared from fructose and glucose precursor were shown in Figure 4, the average size of CDs is 9.99±1.50 nm and 4.86±0.78 nm, respectively. Grain size distributions of

CDs (Figure 5) reveal the formation of CDs through hydrothermal carbonization. It was found that hydrothermal carbonization of different precursors could lead to various sizes of CDs due to the difficulty of precursor conversion [16]. By using the different solvent, we observed a slightly difference of CDs size when synthesized using the same sucrose precursor.
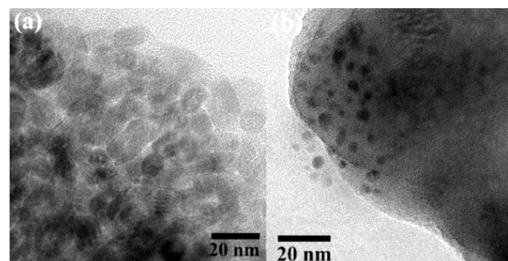
Figure 4. TEM images of CDs synthesized using (a) fructose precursor and (b) glucose precursor in diluted acetone.

3.2 UV-Visible spectroscopy

UV-Visible absorption spectra of CDs synthesized using a different % weight of disaccharide sucrose precursor in 50v/v diluted ethanol (SCET2) are shown in Figure 6. The two absorption peaks located at 229 nm and 283 nm were observed. UV absorption peak at 229 nm correspond to π to π* transition in the conjugated system of C- C and C=C bonds while UV peak at 283 nm is related to n to π* transition of –C=O group [8]. Absorption peaks are independent of the %weight of precursor as the position of peaks remains unchanged with increasing precursor concentration, due to the similar carbon core states and surface functional groups formed by hydrothermal carbonization of sucrose precursor. However, absorption intensity increased as the rising of sucrose concentration due to an increasing amount of CDs core structures and surface functional group in CDs. Furthermore, the main absorption peaks located at 233 nm and 283 nm (Figure 7) were detected by changing to 50%v/v diluted acetone for hydrothermal carbonization of 2%wt sucrose precursor (SCAC2), which are shifted as compared to that for synthesized in diluted ethanol solution. Red shift is observed in π to π* transition (229 nm to 233 nm), revealing a characteristics functional group in solvent media effects to core structures of CDs surrounded by media. Acetone contains carbonyl group in chemical structure while ethanol composes of hydroxyl group, sp^2 carbon core structures of CDs could be tailored due to media solvent, resulting in the shifted peak of C-C and C=C absorption. A disaccharide sucrose composed of two mono-saccharides (glucose and fructose) joined by glycosidic linkage via an ether bond between carbon on the glucosyl unit and carbon on the fructosyl unit. The hydrothermal carbonization process might accelerate the hydrolysis process, converting sucrose into glucose and fructose.
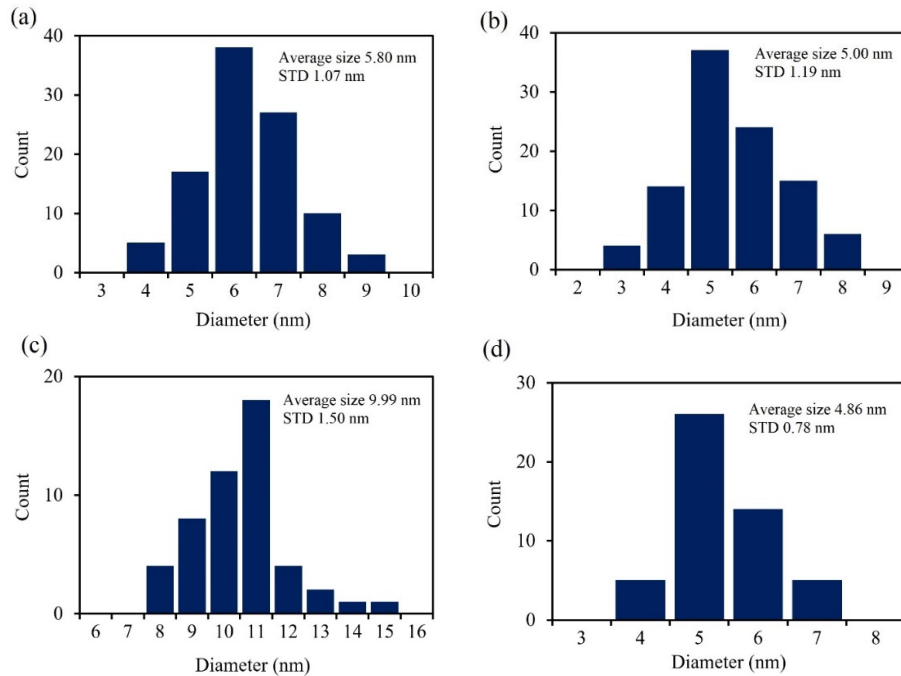
Figure 5. Particle size distributions of CDs synthesized using (a) a sucrose precursor in (a) diluted ethanol (b) a sucrose precursor in diluted acetone (c) a fructose precursor in diluted acetone and (d) a glucose precursor in diluted acetone.

The absorption spectrum of CDs prepared from a monosaccharide fructose in diluted acetone solution (FTAC2) showed similar UV- Vis peaks as CDs synthesized using a sucrose precursor (Figure 8). Interestingly, when CDs were synthesized from monosaccharide glucose precursor with the addition of acetone (GUAC2), different peak appeared at 273 nm for π to π^* transition. The functional groups linked to the surface of CDs prepared from fructose precursor could relate to those found in a carbonized sucrose, which results in similar absorption peaks position. However, the CDs prepared from glucose exhibited different absorption peak position due to another groups including residual hydroxyl groups [13].
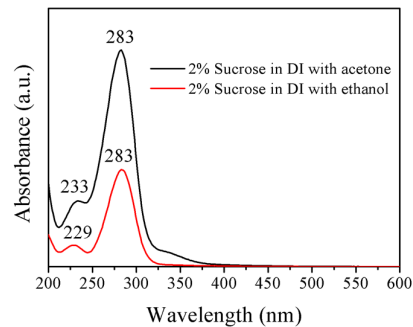
Figure 7. UV- Visible absorption spectra of the CDs synthesized using sucrose in diluted acetone (black) and diluted ethanol (red).
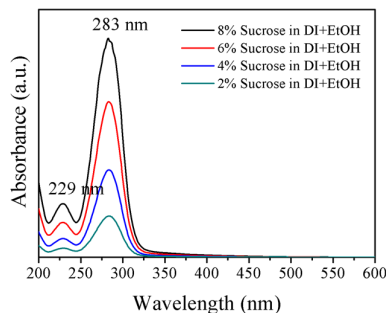
Figure 6. UV-Visible absorption spectra of the CDs using various %weight of sucrose precursor.
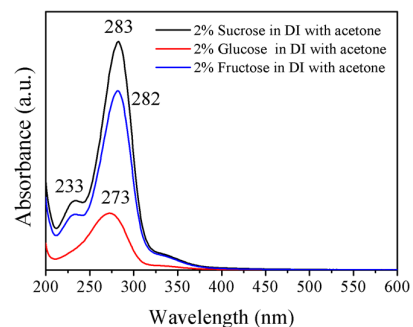

Figure 8. UV- Visible absorption spectra of the CDs synthesized using sucrose (black), glucose (red), and fructose (blue) as precursors.

3.3 Fluorescence spectroscopy

To explore CDs optical properties, FL of the as-prepared CDs was examined using different excitation wavelengths. Emission energy as a function of excitation energy for different CDs is shown in Figure 9. FL spectra of CDs obtained from sucrose (SCET2 and SCAC2) covered blue-to-green wavelength range under excitation from 280 nm- 400 nm. Maximum emission fluorescence could be obtained at 450 nm when excited at 360 nm. Notably, the FL emission depending on the excitation wavelength was also observed in all the CDs samples. Changing the precursor to fructose (FTAC2) and glucose (GCAC2), it was found that the maximum emission of CDs could be tailored to the red-shifted wavelength using excitation wavelength at 380 and 400 nm, respectively. It should be noted that FL properties of CDs prepared from fructose precursor is altered with those prepared from sucrose precursor.

## 3.4 Fourier-transform infrared spectroscopy

FTIR spectra of CDs show functional groups as the results indicated in Figure 10. All prepared CDs composed of C=C functional group as depicted in Figure 11. CDs synthesized from fructose and sucrose precursors are passivated by C=O functional group, which is not found in CDs prepared from a glucose monosaccharide. The broad peaks in the range 3200-3400 cm^{-1} refer to –OH functional group on CDs surface formed during the hydrothermal carbonization of mono- and disaccharide precursor. FTIR results are consistent with UV absorption spectra in which the glucose-derived CDs have more –OH functional group than CDs prepared from fructose and sucrose precursor as represented by the % transmittance.
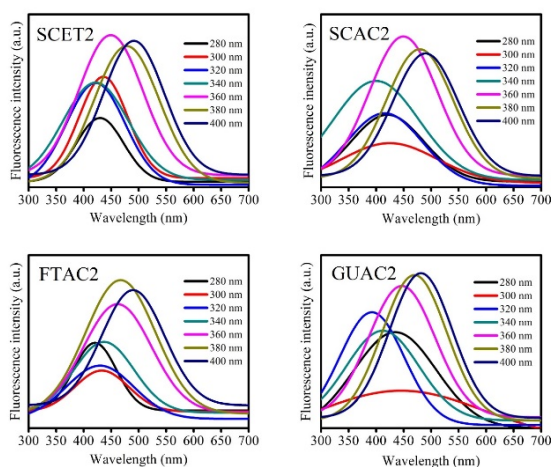
Figure 9. FL spectra CDs excited at the different wavelength.
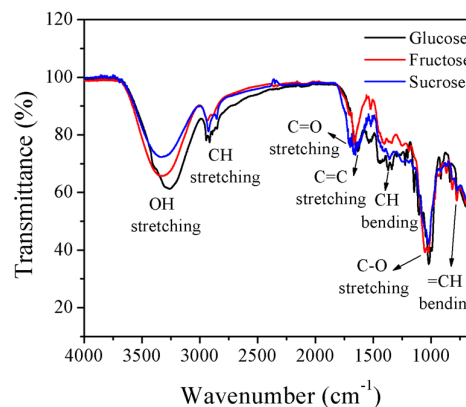
Figure 10. FTIR spectra of the CDs synthesized using glucose (black), fructose (red), and sucrose (blue) precursors.
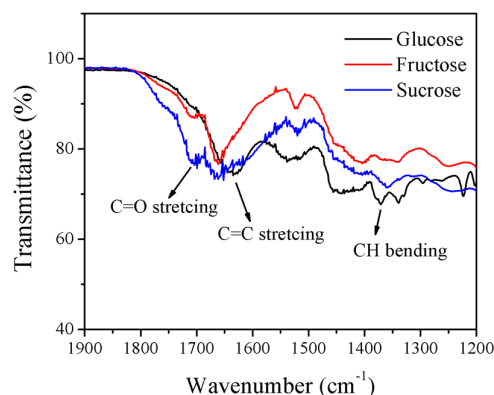
Figure 11. FTIR spectra (1200 – 1900 cm^{-1}) of the CDs synthesized using glucose (black), fructose (red), and sucrose (blue) precursors.

3.5 Cyclic voltammetry

To investigate the oxidation and reduction potentials and their band gaps of CDs, Figure 12 displays the cyclic voltammograms (CV) of CDs prepared from 2% sucrose in a diluted ethanol (SCET2) or diluted acetone (SCAC2) in 2 M H_2SO_4 as an electrolyte, compared with 2 M H_2SO_4 with and without ethanol or acetone. All were done using a typical three-electrode system including a glassy carbon as working electrode, a platinum rod as counter electrode, and a Ag/AgCl in 3 M KCl as reference electrode immersed in 50 ml 2 M H_2SO_4 containing 10 ml sample solution at 50 mVs^{-1}. The CV of SCET2 shows a board oxidation peak at approximately 0.77 V (vs. Ag/AgCl), as seen in Figure 12 (a). Figure 12 (b) displays the CV of SCAC2 showing the three oxidation peaks at, 0.38V, 0.57V , 0.86V (vs. Ag/AgCl) and a strong reduction peak at 0.317V (vs. Ag/AgCl), while the using 2 M H_2SO_4 with and without diluted ethanol or

diluted acetone does not show any oxidation and reduction peaks. It is surprising that the CDs prepared from sucrose with ethanol or acetone reveal electrochemical properties. The highest occupied molecular orbital (HOMO) and the lowest unoccupied molecular orbital (LUMO) level of the CDs can be calculated from the oxidation peaks of CV results using the following equations;

$$E_{HOMO} = -(4.88 - E_{1/2,FC,FC+} = E_{OX}) \qquad (1)$$

$$E_{LUMO} = E_{HOMO} + E_{0-0} \qquad (2)$$

where E_{OX} is the oxidation potential of carbon nanodot, $E_{1/2,FC,FC+}$ is the half- wave potential of FC/FC+ (~0.54 eV), E_{0-0} is the 0-0 energy defined as the lowest energy transition estimated from fluorescence emission spectra results (2.76 eV at λ = 450 nm). The HOMO energy of SCET2 has a value of -5.11 eV corresponding to the oxidation peak labeled as $Ox_{1,et}$, while its LUMO energy is -2.06 eV. The three HOMO energies of SCAC2 have values of -4.72 eV, -4.91 eV, -5.20 eV, while its LUMO energies are obtained as -1.957 eV, -2.154 eV, and -2.441 eV, corresponding to the three oxidation peaks labeled as $Ox_{1,ac}$, $Ox_{2,ac}$, and $O_{x3,ac}$, respectively, as shown in Figure 12 (b). These HOMO and LUMO values of our materials are higher than the MAPI perovskite valence band (VB) (HOMO = -5.5 eV and LUMO = -3.75 eV), which ensure efficient hole transport from the perovskite to the carbon nanodot [7]. The E_{HOMO} and E_{LUMO} of as- prepared CDs compared with MAPI perovskite are summarized in Table 2.

Table 2 E_{HOMO} and E_{LUMO} of CDs compared with MAPI perovskite

| Samples	E_{HOMO} (eV)	E_{LUMO} (eV)
SCET2	-5.11	-2.06
SCAC2	-4.72,	-1.96,
	-4.91,	-2.15,
	-5.20	-2.44
MAPI perovskite	-5.50	-3.75

4. Conclusions

Carbon nanodots (CDs) have been successfully prepared from natural mono disaccharide and disaccharide precursors using a facile hydrothermal carbonization. The absorption spectra of CDs suggested that an increasing in absorption was strongly correlated to the concentration of precursor in a diluted solution. CDs synthesized using a sucrose precursor were found to possess the blue fluorescence with the excitation and maximum emission wavelength at 360 nm and 450 nm, respectively. CDs exhibit excitation wavelength- dependent emission properties because of the surface functional groups inherited from a precursor. The various type of functional groups in precursor could change surface charge distribution of CDs, resulting in different maximum emission properties of CDs. Oxidation, reduction potentials and band gaps of CDs were also analyzed using the cyclic voltammograms (CV). Based on the critical results reported in this study, they clearly suggested that the CDs can be used as a hole transporting material in perovskite solar cell.

5. Acknowledgements

References

[1]   D. R. S. Souza, L. D. Caminhas, J. P. Mesquita, and F. V. Pereira, "Luminescent carbon dots obtained from cellulose," *Materials Chemistry and Physics*, vol. 203, pp. 148-155, 2018.
[2]   R. Miao, Z. Luo, W. Zhong, S. Chen, T. Jiang, B. Dutta, Y. Nasr, Y. Zhang, S., and L. Suib, "Mesoporous TiO_2 modified with carbon quantum dots as a high- performance visible light photocatalyst," *Applied Catalysis B: Environmental*, vol. 189, pp. 26-38, 2016.
[3]   A. Gupta, N. C. Verma, S. Khan, S. Tiwari, A. Chaudhary, and C. K. Nandi, "Paper strip based and live cell ultrasensitive lead sensor using carbondots synthesized from biological media," *Sensors and Actuators B*, vol. 232, pp. 107-114, 2016
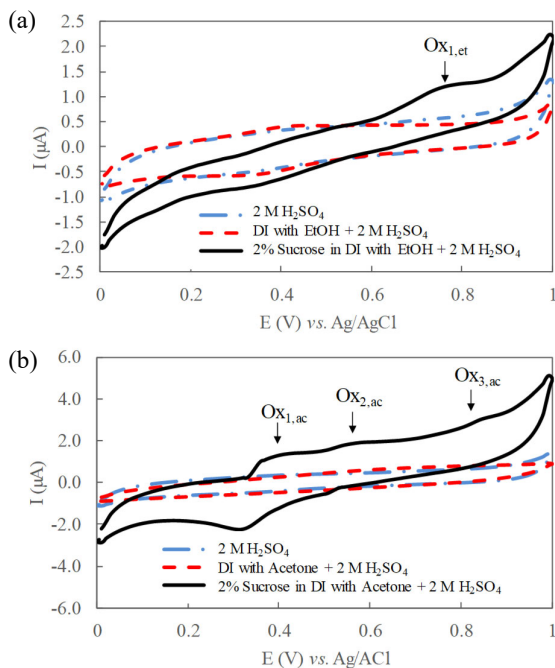
Figure 12 Cyclic voltammograms of CDs prepared from a 2%wt sucrose precursor (a) in diluted ethanol (SCET2) and (b) diluted acetone (SCAC2) in 2 M H_2SO_4 as electrolyte at 50 mVs^{-1}

[4] T. V. Tam, N. B. Trung, H. R. Kim ,J. S. Chung, and W. M. Choi, "One-pot synthesis of N- doped graphene quantum dots as a fluorescent sensing platform for Fe3+ ions detection," *Sensors and Actuators B*, vol. 202, pp. 568-573, 2014.

[5] Y. Wang, L. Bao, Z. Liu, and D. Pang, "Aptamer Biosensor Based on Fluorescence Resonance Energy Transfer from Upconverting Phosphors to Carbon Nanoparticles for Thrombin Detection in Human Plasma," *Analytical Chemistry*, vol. 83, pp. 8130-8137, 2011.

[6] J. Hou, G. Dong, Z. Tian, J. Lu, Q. Wanga, S. Ai, and M. Wang, "A sensitive fluorescent sensor for selective determination of dichlorvos based on the recovered fluorescence of carbon dots-Cu(II) system," *Food Chemistry*, vol. 202, pp. 81-87, 2016.

[7] S. Paulo, G. Stoica, W. Cambarau, E. M. Ferrero, and E. Palomares, "Carbon quantum dots as new hole transport material for perovskite solar cells," *Synthetic Metals*, vol. 222, pp. 17-22, 2016.

[8] H. K. Sadhanala, J. Khatei, and K. K. Nanda, "Facile hydrothermal synthesis of carbon nanoparticles and possible application as white light phosphors and catalysts for the reduction of nitrophenol, *RSC Advances Communication*, vol. 4, pp. 11481-11485, 2014.

[9] G. Panomsuwan, N. Saito, and T. Ishizaki, "Electrocatalytic oxygen reduction activity of boron- doped carbon nanoparticles synthesized via solution plasma process," *Electrochemistry Communications*, vol. 59, pp. 81-85, 2015.

[10] J. F. Y. Fong, S. F. Chin, and S. Muk Ng, *"*Facile synthesis of carbon nanoparticles from sodium alginate viaultrasonic- assisted nano-precipitation and thermal acid dehydrationfor ferric ion sensing," *Sensors and Actuators B*, vol. 209, pp. 997-1004, 2015.

[11] S. Yao, Y. Hu, and G. Li, "Flowing electrolytic synthesis of fluorescent carbon nanoparticles and carbon nanosheets," *Electrochimica Acta*, vol. 155, pp. 305-311, 2015.

[12] P. Suvarnaphaet, C. S. Tiwary, J. Wetcharungsri, S. Porntheeraphat, R. Hoonsawat, P. M. Ajayan, I-M. Tang, and P. Asanithi, "Blue photoluminescent carbon nanodots from limeade," *Materials Science and Engineering C*, vol. 69, pp. 914-921, 2016.

[13] H. Li, X. He, Y. Liu, H. Huang, S. Lian, S. Lee, and Z. Kang, "One-step ultrasonic synthesis of water-soluble carbon nanoparticles with excellent photoluminescent properties," *Carbon*, vol. 49, pp, 605 -609, 2011.

[14] S. Hu, Q. Chang, K. Lin, and J. Yang, "Tailoring surface charge distribution of carbon dots through heteroatoms for enhanced visible- light photocatalytic activity," *Carbon*, vol. 105, pp. 484-489, 2016.

[15] R. Mohan, J. Drbohlavova, and J. Hubalek, "Dual band emission in carbon dots," *Chemical Physics Letters*, vol. 692, pp. 196-201, 2018.

[16] N. Papaioannou, A. Marinovic, N. Yoshizawa, A. E. Goode, M. Fay, A. Khlobystov, M. Titirici, and A. Sapelkin, "Structure and solvents effects on the optical properties of sugar-derived carbon nanodots," *Scientific Reports*, vol. 8, Article number: 6559., 2018.

[17] L. Sai, S. Liu, X. Qian, Y. Yu, and X. Xu, "Nontoxic fluorescent carbon nanodot serving as a light conversion material in plant for UV light utilization," *Colloids and Surfaces B: Biointerfaces*, vol. 169, pp. 422-428, 2018.

[18] R. Wang, X. Wang, and Y. Sun, "One- step synthesis of self-doped carbon dots with highly photoluminescence as multifunctional biosensors for detection of iron ions and pH," *Sensors and Actuators B: Chemical*, vol. 241, pp. 73- 79. 2017.

[19] L. Li, X. Wang, Z. Fu, and F. Cui, "One- step hydrothermal synthesis of nitrogen- and sulfur-co- doped carbon dots from ginkgo leaves and application in biology," *Materials Letters*, vol. 196, pp. 300-303, 2017.